Nuclear Physics B328 (1989) 317–341
North-Holland, Amsterdam

CROSS SECTION FOR FIVE-JET PRODUCTION IN e^+e^- ANNIHILATION*

N.K. FALCK**[1], D. GRAUDENZ** and G. KRAMER

II. Institut für Theoretische Physik der Universität Hamburg, D-2000 Hamburg 50, FRG

Received 8 March 1989
(Revised 1 June 1989)

We describe the calculation of the five-parton production processes $e^+e^- \to q\bar{q}3g$ and $e^+e^- \to 2q2\bar{q}g$ in lowest order QCD perturbation theory. Results for the integrated cross section as a function of the mass resolution cut are presented. We study this cross section also for an abelian vector gluon model. Distributions in various jet variables for standard QCD and for the abelian gluon model are given to see differences between the two models.

1. Introduction

Studies of jet production in electron–positron annihilation at high energies have given us much information about the properties of quarks and gluons and the nature of their interactions as described by quantum chromodynamics (see the following recent reviews as in ref. [1]). Experimental results for the production of up to five jets have been presented by two DESY and one KEK collaboration [2]. In QCD the existence of hadron jets in e^+e^- annihilation results from the primordial production of quarks and gluons and their subsequent fragmentation into hadrons. The first step, the annihilation of e^+ and e^- into quarks and gluons is calculated in QCD perturbation theory. So in lowest order ($O(\alpha_s^0)$) only $q\bar{q}$ states can occur, in $O(\alpha_s)$ the final state is $q\bar{q}g$ and in $O(\alpha_s^2)$ we have the production of $q\bar{q}2g$ and $2q2\bar{q}$ states. The cross sections for the production of these states have been calculated in the past including higher order QCD corrections ($O(\alpha_s^2)$) for no (total inclusive), two, three and four jets. Results in $O(\alpha_s^3)$ exist for σ_{tot} [3]. In third order perturbation theory ($O(\alpha_s^3)$) tree diagrams contribute to 5-jet production. The $O(\alpha_s^3)$ virtual

* Dedicated to Prof. H. Schopper on the occasion of his 65th birthday.

** Supported by Bundesministerium für Forschung und Technologie, 05 4HH92P/3, Bonn, FRG.

[1] Present address: BASF AG, Abteilung ZXT, D-6700 Ludwigshafen, FRG.

0550-3213/89/$03.50

corrections give, together with $O(\alpha_s^3)$ tree level contributions in unresolved regions, the higher order QCD corrections to two, three, and four jets. The calculation of these higher order corrections is very difficult and has not been done yet. On the other hand, the calculation of the tree level diagrams in third order is in some sense straightforward and first results have been presented recently [4].

Besides needing the $O(\alpha_s^3)$ tree diagram results for the calculation of higher order corrections to ($n \leqslant 4$)-jet cross sections, the cross section for 5-parton production is of interest by itself. At PETRA energies the 5-jet rate as measured by the JADE and TASSO collaborations [2], being of the order of 1%, depending on the resolution cut, is certainly larger than the production coming from $O(\alpha_s^2)$ perturbation theory where part of the 4-parton final states contribute to five jets through subsequent fragmentation of quarks and gluons into hadrons [2]. This deficiency in the 5-jet rate is attributed to the production of five partons. We showed in ref. [4] that the difference between the $O(\alpha_s^2)$ results and the measured 5-jet rate can be reasonably well accounted for by the additional cross section for 5-parton production. At PETRA energies the 5-jet cross section could be measured only for sufficiently large resolution cut $y > 0.02$ ($y = m^2/q^2$, where $\sqrt{q^2}$ is the total c.m. energy), which corresponds to an invariant mass cut m of more than 5 GeV. For smaller mass cuts jets cannot be resolved anymore due to the fluctuations in the jet spread caused by fragmentation. At higher energies, in the range of the forthcoming e^+e^- colliders SLC and LEP, the non-perturbative jet spread will be much smaller, so that data at much smaller resolution cuts (down to $y = 0.0025$ which corresponds to $m = 5$ GeV at $\sqrt{q^2} = 100$ GeV) will be obtainable for which the 5-jet rate is appreciable.

The full gauge structure of QCD shows up only in higher than first order. In $O(\alpha_s^2)$ the 3-gluon vertex comes in. Unfortunately the contribution of the non-abelian terms, proportional to N_c^2, in the 4-jet cross section is rather small, so that unique features of the 3-gluon vertex could not be verified yet. In $O(\alpha_s^3)$ the 4-gluon vertex appears in addition. So we might expect that for 5-jet production the non-abelian contributions might be stronger. Of course, this will be of interest only for the analysis of data obtained with SLC or LEP.

The outline of the paper is as follows. In sect. 2 we describe the framework of our calculation and present results for the integrated 5-parton cross section for the two possible final states, (a) for full QCD, (b) in the $N_c \to \infty$ approximation for all diagrams and (c) for an abelian gluon model. In sect. 3 we give predictions for various distributions of common jet variables like sphericity, thrust and acoplanarity and test them whether they show differences between standard QCD and the abelian gluon model.

Some technical details like colour factors for the many contributions are relegated to appendices. Complete cross section formulas cannot be presented because they consist of too many lines. Instead we shall publish the REDUCE programs from which they can be obtained [5]. In sect. 4 we summarize and add some concluding remarks.

2. Integrated five-jet cross section

To order α_s^3 the 5-jet cross section is given by the two sets of diagrams shown in fig. 1 corresponding to the final (jet) states

$$e^+e^- \to q(p_1)\bar{q}(p_2)g(p_3)g(p_4)g(p_5), \tag{1}$$

$$e^+e^- \to q(p_1)\bar{q}(p_2)q(p_3)\bar{q}(p_4)g(p_5). \tag{2}$$

The p_i denote the momenta of the produced partons, quarks q, antiquarks $\bar{q}$ or gluons g. The quarks are assumed to be massless. In (2) the two groups of quarks and antiquarks may have equal or different flavour. The differential cross section is given by

$$d\sigma = \frac{e^4}{2q^6 N_s} l^{\mu\nu} \prod_{i=1}^{5} \frac{d^3 p_i}{2p_{i0}(2\pi)^3} (2\pi)^4 \delta^{(4)}\left(p_+ + p_- - \sum_{i=1}^{5} p_i\right) H_{\mu\nu}, \tag{3}$$

where $q = p_+ + p_-$. For unpolarized beams and for single photon exchange

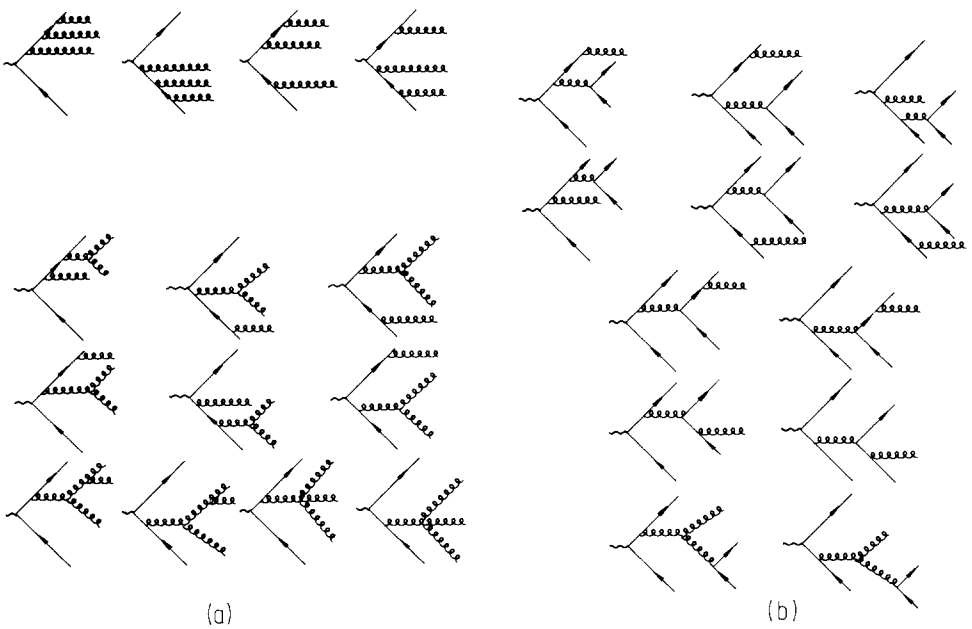

Fig. 1. Feynman diagrams for the production of five partons. (a) Production of $q\bar{q}3g$: all necessary permutations of the gluon lines have to be included, (b) production of $2q2\bar{q}g$: all permutations of the quark and of the antiquark lines have to be included.

(Z exchange can be included in an obvious way) the lepton tensor $l^{\mu\nu}$ is

$$l^{\mu\nu} = p_+^\mu p_-^\nu + p_-^\mu p_+^\nu - \tfrac{1}{2} g^{\mu\nu} q^2. \tag{4}$$

The hadron tensor $H_{\mu\nu}$ contains summations over the final spin, colour and flavour states including the quark charge factors. N_s is a statistical factor due to identity of final state particles which is equal to 6 for (1) and equal to 4 for (2). For (2) we sum over all quark and antiquark flavours in the final state and consider only distributions for such jet variables in which the flavour of the quark or the antiquark is not specified. Then we have the same statistical factor as in the one-flavour case (see also appendix A). The cross section (3) depends on two angle variables which determine the orientation of the "hadronic" 5-jet event relative to the lepton beam direction. We can integrate over these angles. This is equivalent to replacing the lepton tensor (4) by

$$l^{\mu\nu} \to -\tfrac{1}{3} g^{\mu\nu} q^2. \tag{5}$$

In the following we shall consider only cross sections where the angular dependence with respect to the beam direction is integrated out. Then we need only the trace of the hadron tensor $H_{\mu\nu}$. We write $H_{\mu\nu}$ in the following form

$$H_{\mu\nu} = (4\pi\alpha_s)^3 \sum_{k=1}^{N_f} Q_k^2 \sum_{m \geqslant n = 1} A(m, n)_{\mu\nu}. \tag{6}$$

$A(m, n)$ stands for the sum of products of diagram m with diagram n and of n with m (except for $m = n$) taken from the list of diagrams in fig. 1, summed over spins, colours and flavours of the final state (1) and (2). For example, the class of the QED-type diagrams, the first four diagrams in fig. 1 together with the permutations of the final three gluon lines, consists actually of 24 graphs, so that the sum in eq. (6) runs from $m = 1$ to $m = 24$ in this case. Similarly, the class of QCD-type diagrams, i.e. the second group of diagrams in fig. 1 with permutations of final gluon lines consists of 30 diagrams, whereas for the final state (2) we have in total 48 diagrams.

The calculation of the traces of the matrix element $A(m, n)_{\mu\nu}$ was performed in the Feynman gauge. To sum over gluon polarisations we have taken the trace with respect to the gluon polarisation index. Then it is necessary to cancel the contribution from the unphysical scalar and longitudinal gluon polarisations by adding ghost terms. In total there are 72 ghost diagrams whose products must be added in eq. (6). This procedure is well known [6] and was also used for the calculation of the $e^+e^- \to q\bar{q}2g$ process [7]. In order to ensure that the ghost terms have the correct structure to cancel the unwanted polarisation of the final gluons, we have checked the Slavnov–Taylor identity for each of the gluons. Details are described in

appendix B. An alternative procedure to compensate the scalar and longitudinal gluon terms is described in ref. [8]. For technical reasons this procedure could not be applied to our case, since for this method to work it would have been necessary to calculate the full tensor and not just the trace concerning gluon polarisations, which needs much more storage.

The calculations of the many traces for summation over quark and gluon polarisations have been done with REDUCE. The matrix elements come out as functions of the invariants $2p_ip_j$ $(i, j = 1,\ldots,5)$ and the colour factors which have been calculated by hand. The colour factors for all products of diagrams are given in appendix A. The expressions obtained for $A(m, n)^{\mu}_{\mu}$ are too long to be reproduced here. We have made several checks to make sure that the results show the expected behaviour. For this purpose we have chosen invariants in the infrared or collinear region and have verified that the matrix elements show the expected scaling if some invariants are decreased. No attempt was made to find out whether several matrix elements could be combined so that some terms would cancel each other and so the resulting expressions would be shorter. Many matrix elements differ only by permutation of momenta. They could have been taken out if the integration measure is symmetric with respect to permutations of momenta. Although this is the case for all applications in this paper we have not done this so that our formulae can be directly applied in Monte Carlo studies which incorporate the fragmentation of quarks and gluons. The REDUCE output is directly transformed into FORTRAN codes and then used in a Monte Carlo routine for the calculation of the integrated cross section and the single-variable distributions. Other techniques for calculating matrix elements for such complicated final states are described in ref. [9].

To avoid the infrared and collinear singularities present in the tree-level diagrams we have introduced an invariant mass cutoff. With this we accept only those contributions of the total 5-parton phase space for which all $y_{ij} = 2p_ip_j/q^2 > y$. We have calculated $\sigma_{5\text{-jet}}(y)/\sigma_0$, where σ_0 is the zeroth order cross section $\sigma_0 = 4\pi\alpha^2\Sigma_k Q_k^2/q^2$, with a fixed value of $\alpha_s = 0.2$. Since the 5-jet cross section is proportional to α_s^3, our results can easily be transformed to other values of the coupling constant. Except for the factor α_s^3 the cross sections normalised by σ_0 are independent of q^2.

First we have calculated $\sigma_{5\text{-jet}}(y)/\sigma_0$ for $y = 0.005$, 0.01, 0.02, 0.03 and 0.04 with the complete matrix elements according to standard QCD, i.e. $C_F = 4/3$ and $N_c = 3$, and with $N_f = 5$. The results are shown in fig. 2 where the 5-jet rate is plotted as a function of y. In this logarithmic plot, the 5-jet rate increases approximately linearly with decreasing y. For $y = 0.005$ the rate is appreciable, equal to 19% with $\alpha_s = 0.2$. For $y \to 0$ we expect $\sigma_{5\text{-jet}}(y)$ to diverge like $\log^6 y$ due to the infrared singularities. Below $y = 0.0025$ the 5-jet rate is above 100%, so that for such small y the perturbative cross section with fixed order α_s becomes meaningless. For $y > 0.005$ we consider our results as reliable estimates of the 5-jet cross section.

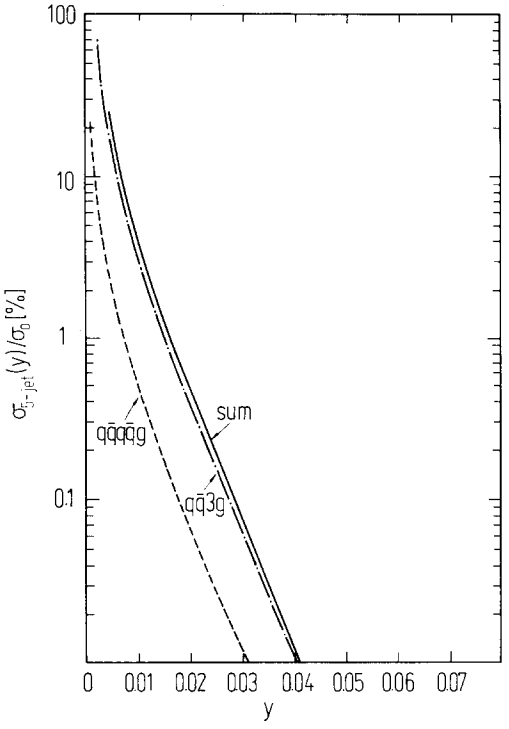

Fig. 2. 5-jet rate in % versus invariant mass cutoff y. (a) $q\bar{q}3g$ final state: dashed–dotted line, (b) $2q2\bar{q}g$ final state: dashed line, (c) sum of (a) and (b): full line.

Secondly we considered the following approximation in the matrix elements. For N_c being large we have $C_F = \frac{1}{2}N_c$, so that terms proportional to $C_F - \frac{1}{2}N_c = -1/2N_c$ are small compared to the dominant terms. To test the large N_c approximation, we have recalculated the integrated cross section with the approximation that all terms proportional to $C_F - N_c/2$ are neglected and terms proportional to $C_F - N_c/4$ are multiplied with $N_c/4$ instead. Otherwise $C_F = 4/3$ and $N_c = 3$. The results in this large N_c limit approximation are compared with the full calculation in fig. 3 by plotting the ratio of the large N_c approximation to the full theory separately for the $q\bar{q}3g$ and $2q2\bar{q}g$ final states. This ratio is equal to 1.13 for $q\bar{q}3g$ and somewhat smaller for $2q2\bar{q}g$. It tends to 1 for $y \to 0$ as one expects. The $N_c \to \infty$ approximation is a good estimate of the full cross section. But with our method of calculating the cross section the formulae are not simplified very much so that the large N_c approximation is of no significant advantage over the complete expressions.

The ratio of cross sections for $2q2\bar{q}g$ and for $q\bar{q}3g$ is also exhibited in fig. 3. It decreases for $y \to 0$ as expected since $2q2\bar{q}g$ is less infrared singular than $q\bar{q}3g$. This ratio is 0.19 for $y = 0.04$ and equal to 0.11 for the smallest $y = 0.001$ plotted. This

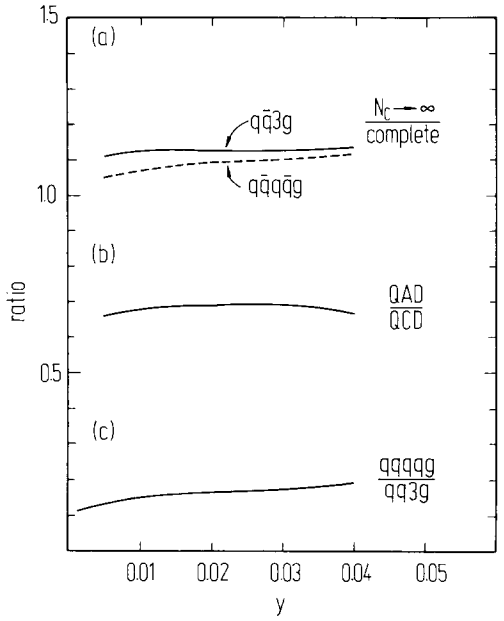

Fig. 3. Ratio of 5-jet rates versus invariant mass cutoff y. (a) ($N_c \to \infty$/complete) for $q\bar{q}3g$ final state and $2q2\bar{q}g$ final state, (b) ratio of 5-jet rates for QAD and QCD, (c) ratio of 5-jet rates for $q\bar{q}3g$ and $2q2\bar{q}g$ final states in full QCD.

ratio is larger than that obtained in the 4-jet case for the ratio of the $2q2\bar{q}$ and the $q\bar{q}2g$ cross sections [7, 10].

It is interesting to note that the recently published third order term in σ_{tot}/σ_0 is 0.0166 with $\alpha_s = 0.2$ [3]. This means that even for $y = 0.01$ the $\sigma_{5\text{-jet}}(y)/\sigma_0$ is of the same order of magnitude as the constant term in σ_{tot}/σ_0. In general one would expect that $\sigma_{5\text{-jet}}/\sigma_0$ should be much larger than the third order term of σ_{tot}/σ_0 since it contains a series of y-dependent terms proportional to $\log^n y$ ($n = 1, \ldots, 6$). This shows that there must be cancellations of terms in $\sigma_{5\text{-jet}}/\sigma_0$ or/and that the $O(\alpha_s^3)$ term in σ_{tot}/σ_0 is exceptionally large.

The comparison with an abelian gluon theory, called QAD here, is done following ref. [10] by replacing the terms proportional to N_c^2 by zero but keeping $C_F = 4/3$, so that the abelian coupling constant is equal to $\alpha_a = C_F\alpha_s$. With the abelian coupling defined in this way we have the same cross section for 3-jet production, $e^+e^- \to q\bar{q}g$, as in QCD in lowest order of α_s. The contribution of the final state (2) is treated in the same way with $N_f = 5$. To have the same zeroth order cross section as in QCD it is actually necessary to increase the number of flavours by a factor of 3. This has not been done consistently. Instead, we normalize the cross section with the same σ_0 as in QCD, but have not increased the number of flavours in the intermediate fermion "loops" accordingly (see refs. [7, 11] for a different treatment

in 4-jet production). Since (2) contributes only a small fraction to the cross section, this inconsistency is not relevant. Actually it will be difficult to distinguish QAD from QCD alone on the basis of the absolute value of the cross section for a special y value. Therefore our results for $\sigma_{5\text{-jet}}/\sigma_0$ serve more for the purpose of normalisation of the single-variable distributions to be considered in sect. 3. The resulting 5-jet cross section for the abelian gluon model (QAD) divided by the full QCD cross section is also shown as a function of y in fig. 3. The difference between the full QCD curve and the QAD curve is a measure of the influence of the 3- and 4-gluon couplings (and other non-abelian terms of course). The separation of the 3- and 4-gluon contributions from all other terms can be done only for a particular gauge and therefore is a gauge dependent result. For this reason we consider the comparison between QCD and QAD as defined above much more meaningful. The ratio QAD/QCD is approximately 0.7. This means that the genuine QCD type contributions, which are proportional to $N_c^2 C_F^2$ make an appreciable contribution to the cross section. This is different in the 4-jet case where the non-abelian $N_c^2 C_F$ part is much smaller, approximately 12% of the $N_c C_F^2$ term for the range of y's considered in this paper [7]. Since for five jets the non-abelian contributions are much larger, it will be easier to verify these terms experimentally, for example, by measuring such observables which enhance the non-abelian contributions further.

Above we saw that the non-abelian contributions are significant for 5-jets. So it is of interest to find out which type of diagrams gives the major contributions to the integrated cross section. For this purpose we have done the integrations for the following groups of diagrams separately: (1) QED-type diagrams, (2) diagrams with one or two 3-gluon vertices and (3) diagrams with the 4-gluon vertex. Then the contribution of all QED-type diagrams is denoted (1–1), the interference between group (1) and group (2) is called (1–2) and so on. We have calculated the separate contributions of (1–1), (1–2), (2–2), (1–3), (2–3), (3–3) and of the ghost terms to $\sigma_{5\text{-jet}}/\sigma_0$. The results (in %) for $y = 0.01, 0.02, 0.03, 0.04$, together with the sum of all

TABLE 1
Contributions to $\sigma_{5\text{-jet}}/\sigma_0$ in % originating from different diagram combinations (1–1), (1–2), (2–2), (1–3), (2–3), and (3–3) and ghost for various cut values y. (1) stands for QED-type, (2) for diagrams with 3-gluon vertices and (3) for diagrams with a 4-gluon vertex.

y	0.01	0.02	0.03	0.04
ghost	−0.038	−0.0051	−0.00084	−0.00014
(1–1)	0.32	0.042	0.0070	0.0011
(1–2)	1.99	0.25	0.043	0.0068
(2–2)	1.16	0.12	0.019	0.0027
(1–3)	−0.058	−0.0067	−0.00094	−0.00014
(2–3)	0.17	0.023	0.0035	0.00059
(3–3)	0.0088	0.0015	0.00026	0.00005
sum	3.56	0.42	0.071	0.012

contributions, which agrees with the result in fig. 2, is given in table 1. We see that the ghost contributions are really negligible. The main contributions come from (1–1), (1–2) and (2–2). All the others are negligible. The largest term comes from the interference of (1) with (2). We also notice that the 4-gluon vertex makes only a small contribution. The largest of them is (2–3) which is roughly 50% of (1–1). Table 1 also tells us that the sum of (1–1), (1–2) and (2–2) is sufficient for obtaining a good estimate of the 5-jet rate.

3. Jet-variable distributions

The differential cross section for 5-jet production depends on many variables even after the integrations over θ and χ have been done. Eventually it may be useful to study distributions on several of these 5-parton or 5-jet variables. In this section we shall single out one jet variable, as for example acoplanarity, thrust or sphericity, and study differential distributions in one of them. We start with acoplanarity A whose definition is well known [7]. Final states with more than 3 jets are characterized by a non-vanishing A. Therefore, on the parton level, non-vanish-

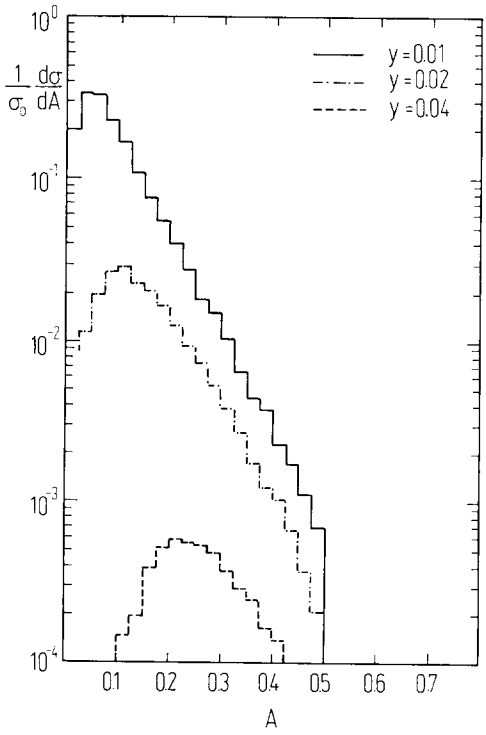

Fig. 4. Acoplanarity distribution of 5-parton production for $y = 0.01$, $y = 0.02$ and $y = 0.04$.

ing A distinguishes 4 and more jets from 2 and 3 jets. In cluster analysis the deficiency of 4-cluster events as compared to $O(\alpha_s^2)$-QCD predictions has been particularly noticed in the A distribution, where the cross section for larger A is experimentally larger than predicted [2]. If this has something to do with 5-parton production it is of interest to know the A distribution for this final state.

One possibility to confront our predictions with experimental results, being produced in the future with SLC or LEP, would be on the basis of a cluster analysis of the hadronic final state as has been done for PETRA and TRISTAN data [2]. Under the assumption that the multi-cluster events are reasonably good representatives for multi-jet events one can compare jet variable distributions of the 5-cluster events with the distributions of the 5-parton final state, of course with the same cuts applied as in the cluster analysis. Before this could be done, it is necessary to know that the 5-cluster distributions are not disturbed too much by the hadronisation, which could be checked by adding the fragmentation of quarks and gluons to the 5-parton production in the same way as for 2-, 3- and 4-parton production in the past [1,2]. For such a comparison we have calculated the distributions in the variables acoplanarity A, thrust T and sphericity S for final states with fixed resolution cuts $y = 0.04$, 0.02 and 0.01. The results for $\sigma_0^{-1}\,\mathrm{d}\sigma/\mathrm{d}A$, $\sigma_0^{-1}\,\mathrm{d}\sigma/\mathrm{d}T$ and

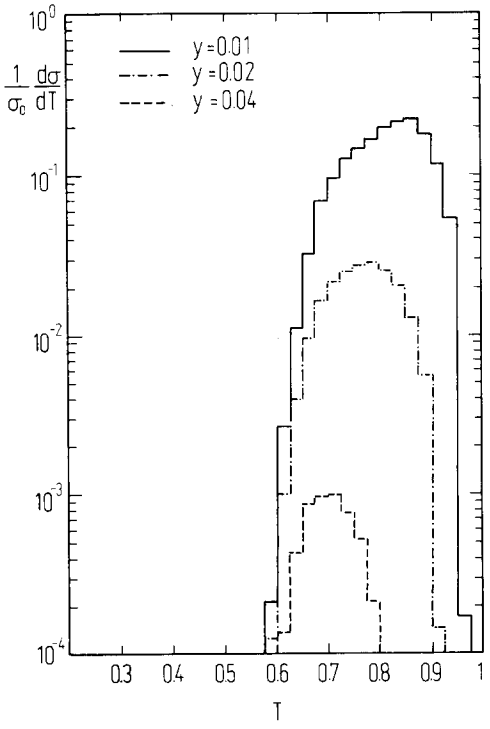

Fig. 5. Thrust distribution of 5-parton production for $y = 0.01$, $y = 0.02$ and $y = 0.04$.

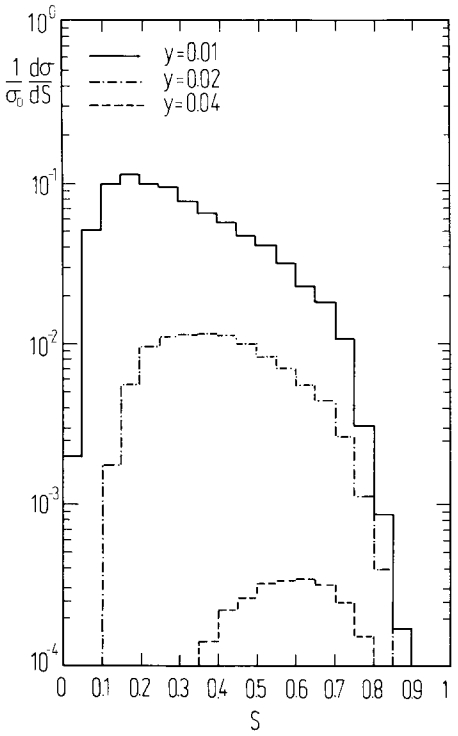

Fig. 6. Sphericity distribution of 5-parton production for $y = 0.01$, $y = 0.02$ and $y = 0.04$.

$\sigma_0^{-1}\,d\sigma/dS$ are plotted in figs. 4, 5 and 6, respectively. The integrals over the curves in these figures yield the cross sections $\sigma_0^{-1}\sigma_{5\text{-jet}}(y)$ shown in fig. 2. The minima near $A = 0$, $T = 1$ and $S = 0$ are caused by the resolution cut y. Due to this cut the maxima of the curves shift with increasing y to larger A, smaller T and larger S. The normalisation of the curves for $y = 0.04$ is very much reduced. Therefore, only the distributions with smaller y cuts are likely to be studied experimentally.

We have seen above that the cross section for the abelian theory is reduced significantly when the coupling is held fixed to yield the same $q\bar{q}g$ cross section. But also the shape of the distribution changes. In fig. 7 we show the acoplanarity distribution for $y = 0.01$ for the full QCD and for the abelian theory QAD. For this case the integrated cross sections differ by a factor 1.5, but in the tail the QAD distribution is reduced by a factor 2.0 compared to the QCD distribution. This means that the abelian distribution falls off somewhat faster than the non-abelian distribution. The same qualitative behaviour occurs in the thrust distribution in fig. 8; the tail for small T is reduced more than the maximum when compared to the QCD distribution. Such differences can be enhanced by looking at particular variables which are sensitive to the terms having the 3-gluon and 4-gluon couplings.

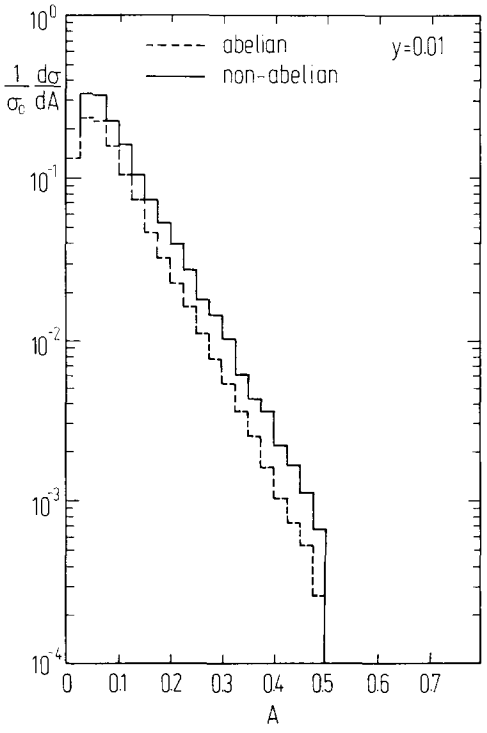

Fig. 7. Acoplanarity distribution of 5-parton production with $y = 0.01$ for full QCD (full line) and QAD (dotted line).

It is obvious that many more variables could be studied. Also measurements of the angular distributions of the 5-jet final state with respect to the beam axis can provide more detailed tests of QCD. But before this is being done it is necessary to supplement the 5-parton cross sections with fragmentation models in order to see how the various distributions look on the level of hadrons which are measured in the experiment.

4. Summary and concluding remarks

We have calculated the 5-jet production processes $e^+e^- \to q\bar{q}3g$ and $e^+e^- \to 2q2\bar{q}g$ in lowest order QCD perturbation theory. The $q\bar{q}3g$ production dominates over the $2q2\bar{q}g$ production. This is similar to 4-jet production where $q\bar{q}2g$ dominates over $2q2\bar{q}$. The contribution of genuine QCD diagrams is appreciable as was found by comparing with an abelian gluon model. This should make it easier to verify the presence of the 3- and 4-gluon couplings.

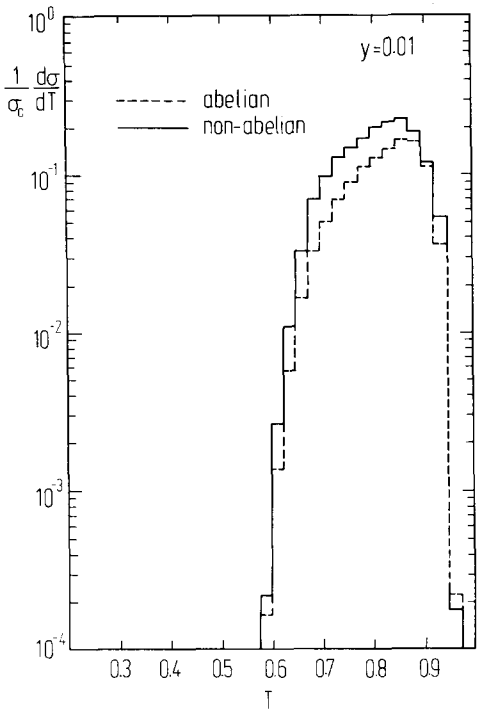

Fig. 8. Thrust distribution of 5-parton production with $y = 0.01$ for full QCD (full line) and QAD (dotted line).

We have given results for the integrated 5-jet cross section as a function of the invariant mass cut. For sufficiently small cut values the 5-jet rate is large, rendering detailed studies of 5-jet production feasible at large enough energies, where the non-perturbative jet spread is very much reduced. We have calculated acoplanarity, thrust and sphericity distributions for various cut values and compared the results for standard QCD and for an abelian gluon model.

An evaluation of the cross section with the approximation that terms of order $1/N_c^2$ compared to 1 are neglected, gives 10% larger cross sections. On the technical side the final formulae from which the cross sections for the final states (2.1) and (2.2) are calculated, based on many diagrams with all their interferences, are very long and cannot be published in a paper but can be reproduced using a REDUCE program which will be published [5].

Our results have been produced for one-photon exchange only, i.e., for a pure vector current. For the high e^+e^- energies of interest to us also Z exchange is present, which has also an axial-vector coupling. In almost all contributions the cross section for the axial-vector current is identical to the vector current. The only exception are those contributions to $e^+e^- \to 2q2\bar{q}g$ with two traces as in fig. 9b.

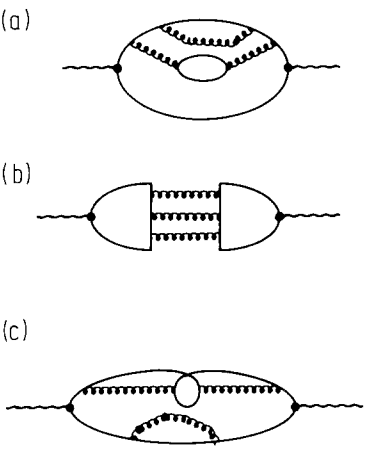

Fig. 9. Product of Feynman diagrams for $2q2\bar{q}g$ production with (a), (b) two traces and (c) one trace.

Since these terms are only a small fraction of the complete $2q2\bar{q}g$ cross section, which by itself is at most only 15% of the total integrated 5-jet cross section, our results can be applied safely also to Z exchange after the multiplication with the known Z propagator instead of the photon propagator has been done.

The formulae which we generated for calculating the 5-jet cross section in e^+e^- annihilation can also be used after crossing to calculate cross sections for other reactions having the same quark and gluon legs, for example to $\gamma q \to q3g$ and $\gamma q \to 2q\bar{q}g$, i.e. 5-jet production in deep inelastic scattering, or to $q\bar{q} \to 3g\gamma$ and $q\bar{q} \to q\bar{q}g\gamma$, i.e. multi-jet production in the Drell–Yan process, in direct photon production or in W/Z production.

Appendix A

COLOUR FACTORS

In this appendix we collect the results for the colour factors of the various contributions. These colour factors have been calculated directly without the help of REDUCE. In fig. 1 we presented the diagrams without the momentum labels. Therefore these diagrams give the general structure and do not exhaust the complete list of contributing diagrams. The complete list can be generated as follows. Let us begin with the diagrams for the $q\bar{q}3g$ final state. Then we look first at the QED-type diagrams, the first four diagrams in fig. 1. We define the momenta of the four partons in the final state by $e^+e^- \to q(p_1)\bar{q}(p_2)g(p_3)g(p_4)g(p_5)$ as in (1), where the three gluons have momenta p_3, p_4 and p_5, seen from the top. These four diagrams define class I. The colour factor multiplying these diagrams is $-iT^{a_3}T^{a_4}T^{a_5}$. The

complete list of all QED-type diagrams consists of five more classes II, III, IV, V and VI, which are obtained from class I by the following permutations of momenta:

$$\begin{aligned} &\text{II:} && 3 \to 4 \to 5 \to 3, \\ &\text{III:} && 3 \to 5 \to 4 \to 3, \\ &\text{IV:} && 3 \to 4 \to 3, \\ &\text{V:} && 3 \to 5 \to 3, \\ &\text{VI:} && 4 \to 5 \to 4. \end{aligned} \tag{7}$$

These are 24 diagrams. The colour factors in the cross section consist of the colour traces of the products of the corresponding colour factors of the diagrams, for example

$$\text{II}^* = \mathrm{Tr}(T^{a_3}T^{a_4}T^{a_5}T^{a_5}T^{a_4}T^{a_3}) = N_c C_F^3 = CF_1, \tag{8}$$

with $C_F = (N_c^2 - 1)/2N_c$ and $N_c = 3$ for $\mathrm{SU}(3)_{\mathrm{colour}}$. The other products are defined analogously. They are collected in table 2a with the following definitions used

$$\begin{aligned} CF_2 &= N_c C_F \left(C_F - \tfrac{1}{2}N_c\right)^2, \\ CF_3 &= N_c C_F^2 \left(C_F - \tfrac{1}{2}N_c\right), \\ CF_4 &= N_c C_F \left(C_F - N_c\right)\left(C_F - \tfrac{1}{2}N_c\right). \end{aligned} \tag{9}$$

The next group of diagrams has 3-gluon and 4-gluon couplings. The first three of these diagrams in fig. 1, where the 3-gluon coupling is at the top, make up the class a_1, the second three diagrams, where the 3-gluon coupling is at the bottom, are denoted class a_2 and the last four diagrams with two 3-gluon couplings and the diagram with the 4-gluon coupling are denoted class a_3. In a_1, a_2 and a_3 the labelling of the gluon momenta is again p_3, p_4, p_5, always from the top to the bottom. The classes b_1, b_2, b_3 and c_1, c_2, c_3 are generated from the classes a_1, a_2, a_3 by permutations of momenta. So b_1, b_2, b_3 are obtained from a_1, a_2, a_3 by the permutation $3 \to 4 \to 5 \to 3$, and c_1, c_2, c_3 by the permutation $3 \to 5 \to 4 \to 3$. This way we obtain 30 genuine QCD-type diagrams. The permutations of the graph with the 4-gluon vertex come about since we have dissolved the three terms in the 4-gluon vertex which are connected by cyclic permutation into three separate diagrams.

The remaining colour factors come from the interference between the QED-type and the genuine QCD-type diagrams, as for example

$$a_1\text{I}^* = if^{a a_4 a_3}\ \mathrm{Tr}(T^a T^{a_5} T^{a_5} T^{a_4} T^{a_3}) = -\tfrac{1}{2}N_c^2 C_F = -\tfrac{1}{2}CF_5 \tag{10}$$

TABLE 2
Colour factors for $q\bar{q}3g$ contributions. (a) QED-type diagrams: $X \cdot Y^*$ where X, Y run from I to V, the matrix is symmetric. (b) Interference contributions between QED-type and QCD-type diagrams: $a_\alpha \cdot X^*$ etc. where $\alpha = 1,2,3$. (c) QCD-type diagrams: $a_\alpha \cdot a_\beta^*$ etc., $\alpha, \beta = 1,2,3$. The missing entries are obtained as follows: $b_\alpha \cdot b_\beta^* = c_\alpha \cdot c_\beta^* = a_\alpha \cdot c_\beta^*$ and $c_\alpha \cdot b_\beta^* = b_\alpha \cdot a_\beta^*$.

(a)

	I*	II*	III*	IV*	V*	VI*
I	CF_1	–	–	–	–	–
II	CF_2	CF_1	–	–	–	–
III	CF_2	CF_2	CF_1	–	–	–
IV	CF_3	CF_3	CF_4	CF_1	–	–
V	CF_4	CF_3	CF_3	CF_2	CF_1	–
VI	CF_3	CF_4	CF_3	CF_2	CF_2	CF_1

(b)

	I*	II*	III*	IV*	V*	VI*
a_1	$-\frac{1}{2}CF_5$	$\frac{1}{2}CF_7$	$-\frac{1}{2}CF_7$	$\frac{1}{2}CF_5$	$\frac{1}{2}CF_7$	$-\frac{1}{2}CF_7$
a_2	$-\frac{1}{2}CF_5$	$-\frac{1}{2}CF_7$	$\frac{1}{2}CF_7$	$-\frac{1}{2}CF_7$	$\frac{1}{2}CF_7$	$\frac{1}{2}CF_5$
a_3	$\frac{1}{4}CF_6$	0	$-\frac{1}{4}CF_6$	$-\frac{1}{4}CF_6$	$\frac{1}{4}CF_6$	0
b_1	$-\frac{1}{2}CF_7$	$-\frac{1}{2}CF_5$	$\frac{1}{2}CF_7$	$-\frac{1}{2}CF_7$	$\frac{1}{2}CF_5$	$\frac{1}{2}CF_7$
b_2	$\frac{1}{2}CF_7$	$-\frac{1}{2}CF_5$	$-\frac{1}{2}CF_7$	$\frac{1}{2}CF_5$	$-\frac{1}{2}CF_7$	$\frac{1}{2}CF_7$
b_3	$-\frac{1}{4}CF_6$	$\frac{1}{4}CF_6$	0	0	$-\frac{1}{4}CF_6$	$\frac{1}{4}CF_6$
c_1	$\frac{1}{2}CF_7$	$-\frac{1}{2}CF_7$	$-\frac{1}{2}CF_5$	$\frac{1}{2}CF_7$	$-\frac{1}{2}CF_7$	$\frac{1}{2}CF_5$
c_2	$-\frac{1}{2}CF_7$	$\frac{1}{2}CF_7$	$-\frac{1}{2}CF_5$	$\frac{1}{2}CF_7$	$\frac{1}{2}CF_5$	$-\frac{1}{2}CF_7$
c_3	0	$-\frac{1}{4}CF_6$	$\frac{1}{4}CF_6$	$\frac{1}{4}CF_6$	0	$-\frac{1}{4}CF_6$

(c)

	a_1*	a_2*	a_3*
a_1	CF_5	–	–
a_2	$\frac{1}{4}CF_6$	CF_5	–
a_3	$-\frac{1}{2}CF_6$	$-\frac{1}{4}CF_6$	CF_6
b_1	0	CF_7	$\frac{1}{4}CF_6$
b_2	$\frac{1}{4}CF_6$	0	$-\frac{1}{4}CF_6$
b_3	$\frac{1}{4}CF_6$	$\frac{1}{2}CF_6$	$-\frac{1}{2}CF_6$
c_1	0	$\frac{1}{4}CF_6$	$\frac{1}{4}CF_6$
c_2	CF_7	0	$\frac{1}{2}CF_6$
c_3	$\frac{1}{4}CF_6$	$-\frac{1}{4}CF_6$	$-\frac{1}{2}CF_6$

and the products of the QCD-type diagrams with itself. An example is

$$a_1 a_1^* = f^{aa_4a_3} f^{ba_4a_3}\,\mathrm{Tr}\left(T^a T^{a_5} T^{a_5} T^b\right) = N_c^2 C_F = CF_5 . \tag{11}$$

All products are collected in table 2, where the labels of the rows and columns are the classes $\mathrm{I}, \mathrm{II}, \ldots, a_1, a_2, \ldots$ introduced above. In this table two more abbreviations occur:

$$CF_6 = N_c^3 C_F , \qquad CF_7 = N_c^2 C_F \left(C_F - \tfrac{1}{2}N_c\right). \tag{12}$$

In the large N_c limit all contributions proportional to CF_2, CF_3, CF_4 and CF_6 are neglected. This produces an error of approximately 10% in the cross section as already discussed in sect. 2.

The colour factors for the final state $q(p_1)\bar{q}(p_2)q(p_3)\bar{q}(p_4)g(p_5)$ are obtained in the following way. First we consider the special case that the quarks coupling to the

TABLE 3
Colour factors for $2q2\bar{q}g$ final states: (a) $AX \cdot AY^*$, where $X = I,\ldots,V$ and $Y = I,\ldots,V$, (b) $BX \cdot AY^*$, (c) $CX \cdot AY^*$, (d) $DX \cdot AY^*$. The missing entries are obtained from: $BX \cdot BY^* = CX \cdot CY^* = DX \cdot DY^* = AX \cdot AY^*$, $CX \cdot BY^* = DX \cdot AY^*$, $DX \cdot BY^* = CX \cdot AY^*$, $DX \cdot CY^* = BX \cdot AY^*$.

(a)

	AI*	AII*	AIII*	AIV*	AV*
AI	$\frac{1}{2}F_1$	–	–	–	–
AII	$\frac{1}{2}F_2$	$\frac{1}{2}F_1$	–	–	–
AIII	F_2	F_3	$\frac{1}{2}F_1$	–	–
AIV	F_3	F_2	$\frac{1}{2}F_2$	$\frac{1}{2}F_1$	–
AV	$-\frac{1}{4}F_4$	$\frac{1}{4}F_4$	$\frac{1}{4}F_4$	$-\frac{1}{4}F_4$	$\frac{1}{2}F_4$

(b)

	AI*	AII*	AIII*	AIV*	AV*
BI	CF_4	CF_2	CF_3	CF_2	$\frac{1}{2}CF_7$
BII	CF_2	CF_3	CF_2	CF_4	$\frac{1}{2}CF_7$
BIII	CF_3	CF_2	CF_4	CF_2	$-\frac{1}{2}CF_7$
BIV	CF_2	CF_4	CF_2	CF_3	$-\frac{1}{2}CF_7$
BV	$\frac{1}{2}CF_7$	$\frac{1}{2}CF_7$	$-\frac{1}{2}CF_7$	$-\frac{1}{2}CF_7$	0

(c)

	AI*	AII*	AIII*	AIV*	AV*
CI	CF_3	CF_2	CF_4	CF_2	$-\frac{1}{2}CF_7$
CII	CF_2	CF_4	CF_2	CF_3	$-\frac{1}{2}CF_7$
CIII	CF_4	CF_2	CF_3	CF_2	$\frac{1}{2}CF_7$
CIV	CF_2	CF_3	CF_2	CF_4	$\frac{1}{2}CF_7$
CV	$-\frac{1}{2}CF_7$	$-\frac{1}{2}CF_7$	$\frac{1}{2}CF_7$	$\frac{1}{2}CF_7$	0

(d)

	AI*	AII*	AIII*	AIV*	AV*
DI	F_2	F_3	$\frac{1}{2}F_1$	$\frac{1}{2}F_2$	$\frac{1}{4}F_4$
DII	F_3	F_2	$\frac{1}{2}F_2$	$\frac{1}{2}F_1$	$-\frac{1}{4}F_4$
DIII	$\frac{1}{2}F_1$	$\frac{1}{2}F_2$	F_2	F_3	$-\frac{1}{4}F_4$
DIV	$\frac{1}{2}F_2$	$\frac{1}{2}F_1$	F_3	F_2	$\frac{1}{4}F_4$
DV	$\frac{1}{4}F_4$	$-\frac{1}{4}F_4$	$-\frac{1}{4}F_4$	$\frac{1}{4}F_4$	$-\frac{1}{2}F_4$

external current and the quarks coupling to the intermediate gluon (see fig. 1) have the same flavour. The diagrams in fig. 1 with the first $q\bar{q}$ having momenta p_1 and p_2 coupled to the current are distinguished as group AI (diagram 1, 2, 3), group AII (diagram 4, 5, 6), group AIII (diagram 7, 8), group AIV (diagram 9, 10) and group AV (diagram 11, 12). The set with the interchange of momenta $1 \leftrightarrow 3$ is denoted $BI,\ldots,BV$, the set with $2 \leftrightarrow 4$ is called $CI,\ldots,CV$ and the set of diagrams with the interchanges $(1 \leftrightarrow 3, 2 \leftrightarrow 4)$ is called $DI,\ldots,DV$. The products AA*, BB* and DD* give the main contribution and are calculated from a product of two traces, in colour and spin space (see fig. 9a). The interference terms DA* and CB* are also proportional to a product of two traces (see fig. 9b), whereas the interference terms BA*, CA*, DB* and DC* have only one trace as indicated in fig. 9c. The complete list of colour factors is given in table 3 with rows and columns from AI up to DV. For this table new abbreviations have been defined:

$$F_1 = N_c C_F^2, \qquad F_2 = N_c C_F\left(C_F - \tfrac{1}{2}N_c\right),$$

$$F_3 = N_c C_F\left(C_F - \tfrac{1}{4}N_c\right), \qquad F_4 = N_c^2 C_F. \tag{13}$$

Finally we explain the charge and statistical factors which must be taken into account. When both fermion lines have the same flavour, there are two pairs of identical particles and we have the statistical factor 1/4. Classifying the diagrams as A, B, C and D, as introduced above, the total contribution is $|A - B - C + D|^2/4$ where the minus signs are due to the anticommuting fermion fields. This is equal to the sum of the contributions in fig. 9a, b, c with the interference terms in fig. 9c getting an additional minus sign. For this case the charge factor is equal to q_i^2 for each flavour i.

The second possibility, that the flavours of the two quark lines are different, is more complicated. Then we can permute only the quark lines completely, i.e. quark and antiquark together, and we get the statistical factor 1/2. Then the total contribution $|A + D|^2/2$ may be decomposed according to $(|A + D|^2 + |B + C|^2)/4$ as long as the integration measure is symmetric with respect to permutations of momenta, which is the case for all specific calculations done for this paper. The charge factor of the diagonal term in fig. 9a, namely AA*, BB* etc. is equal to $\Sigma_i q_i^2$ $(N_f - 1)$, where N_f is the number of flavours. The non-diagonal terms DA* and CB* in fig. 9b has the charge factor $\Sigma_{i \neq j} q_i q_j$.

The total contribution with N_f flavours is obtained as the sum of contributions with equal and unequal flavours which is $\Sigma_i q_i^2/4$ times the sum of N_f times the terms in fig. 9a plus $(\Sigma_i q_i)^2/\Sigma_i q_i^2$ times the interference term in fig. 9b minus the interference term in fig. 9c. For one-photon exchange the factor $(\Sigma_i q_i)^2/\Sigma_i q_i^2 = 1/11$ for five flavours is small.

Appendix B

GHOST DIAGRAMS AND SLAVNOV–TAYLOR IDENTITY

As already explained in sect. 2 the ghost diagrams are needed in order to compensate for the contributions of the scalar (zero component) and longitudinal gluons which have been introduced by using the simplified sum over gluon spins

$$\sum_\lambda \epsilon^\alpha(k, \lambda)\epsilon^{\beta *}(k, \lambda) = -g^{\alpha\beta}. \tag{14}$$

Although it is straightforward to draw the needed diagrams with ghost pairs, it is instructive to look at the ghost diagrams in connection with the Slavnov–Taylor identity. Let $p_i^{e_l}$ be the e_lth component of p_i, where p_i is the momentum of gluon i $(i = 3, 4, 5)$. Then the Slavnov–Taylor identity (STI) for every $i = 3, 4, 5$ is

$$p_i^{e_l} \cdot \sum(\mathrm{q\bar{q}3g - graphs}) = \sum_{i \neq j} p_j^{e_j} \cdot \mathrm{ghost}(i, j). \tag{15}$$

In eq. (15) ghost(i, j) is obtained from the sum of all $\mathrm{q\bar{q}3g}$ diagrams by replacing gluon line i by the ghost line η and the gluon line j by the antighost line $\bar{\eta}$.

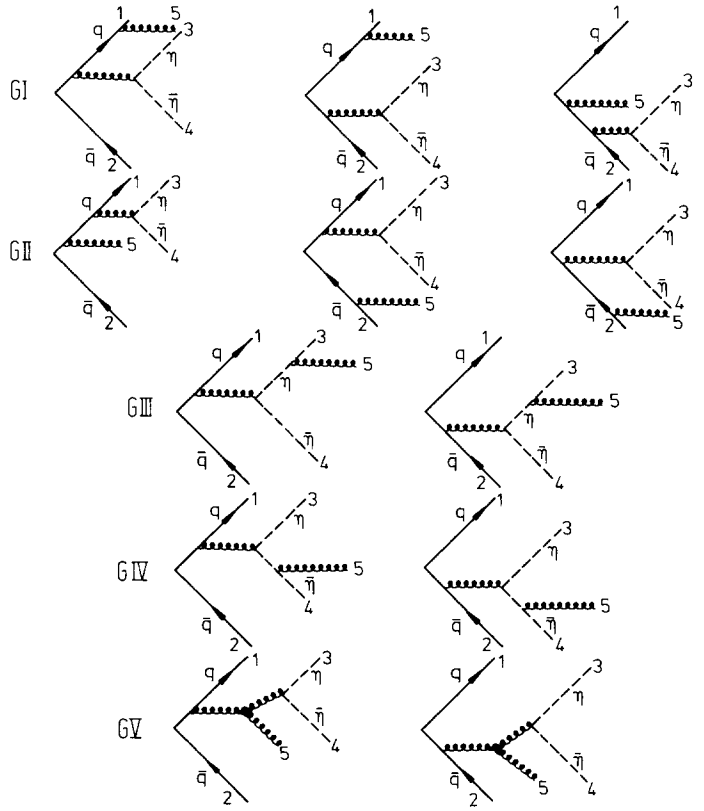

Fig. 10. Feynman diagrams with ghosts for compensation of scalar and longitudinal gluon polarisations needed for gluons with momenta p_3 and p_4.

Therefore, we have six sets of ghost diagrams with $(i, j) = (3,4),(3,5),(4,3),(4,5),$ $(5,3),(5,4)$ which must be added to the already existing diagrams. For $(i, j) = (3,4)$ we have the twelve diagrams shown in fig. 10. They consist of five groups: GI,...,GV, (see table 4) corresponding to the $q\bar{q}3g$ diagrams c_2, a_1, c_3 where in c_3 there are three possibilities how to replace the gluon lines by a ghost and an antighost line. Since η and $\bar{\eta}$ couple to gluons only we need to look in fig. 1 at the diagrams with 3-gluon couplings. All these diagrams are squared, so that there are no interferences between the different sets (i, j). This simplifies the calculation of the colour factors for the ghost contributions. In total we have 72 ghost diagrams, the twelve diagrams in fig. 10 and five times more with different labels for (i, j). In this form the squared ghost diagrams receive also the statistical factor $1/6$ in the same way as for the $q\bar{q}3g$ diagrams because of three identical gluons.

In order to have a check that the ghost terms have been taken into account correctly we have verified eq. (15). Due to the complete symmetry with respect to

TABLE 4
Colour factors for ghost diagrams: GX · GY*, where X = I,...,V and Y = I,...,V.

	GI*	GII*	GIII*	GIV*	GV*
GI	CF_5	–	–	–	–
GII	CF_7	CF_5	–	–	–
GIII	$-\frac{1}{4}CF_6$	$\frac{1}{4}CF_6$	CF_6	–	–
GIV	$-\frac{1}{4}CF_6$	$\frac{1}{4}CF_6$	$-\frac{1}{2}CF_6$	CF_6	–
GV	$\frac{1}{2}CF_6$	$-\frac{1}{2}CF_6$	$-\frac{1}{2}CF_6$	$-\frac{1}{2}CF_6$	CF_6

the three gluon lines it is sufficient to prove the STI for one specific gluon label i, for which we take $i = 3$. Then we have to prove

$$p_3^{e_3} \cdot \sum(\mathrm{q\bar{q}3g - graphs}) = p_4^{e_4} \cdot \mathrm{ghost}(3,4) + p_5^{e_5} \cdot \mathrm{ghost}(3,5). \tag{16}$$

To reduce the l.h.s. of eq. (16) we use the Dirac equation for the massless spinors $\bar{u}(p_1)$ and $v(p_2)$ and the identities

$$\frac{1}{\not p_i}\not p_3\frac{1}{\not p_{i3}} = \frac{1}{\not p_i} - \frac{1}{\not p_{i3}}, \qquad \frac{1}{\not p_{i3}}\not p_3\frac{1}{\not p_i} = \frac{1}{\not p_i} - \frac{1}{\not p_{i3}}, \tag{17}$$

where $p_{i3} = p_i + p_3$. First we multiply the QED-type diagrams I,...,V with $p_3^{e_3}$. The result can be written in terms of commutators of the T^a:

$$\begin{aligned}
&p_3^{e_3} \cdot \sum(\mathrm{QED - type - q\bar{q}3g - graphs}) \\
&= p_3^{e_3} \cdot (\mathrm{I + II + III + IV + V + VI}) \\
&= \bar{u}(p_1)\Bigg\{ f^{aa_3a_4}T^aT^{a_5}\left(\gamma^{e_4}\frac{1}{\not p_{134}}\gamma^{e_5}\frac{1}{\not p_{1345}}\gamma^{\mu} - \gamma^{e_4}\frac{1}{\not p_{134}}\gamma^{\mu}\frac{1}{\not p_{35}}\gamma^{e_5} + \gamma^{\mu}\frac{1}{\not p_{2345}}\gamma^{e_4}\frac{1}{\not p_{25}}\gamma^{e_5}\right) \\
&\quad + f^{aa_3a_5}T^{a_4}T^{a}\left(\gamma^{e_4}\frac{1}{\not p_{14}}\gamma^{e_5}\frac{1}{\not p_{1345}}\gamma^{\mu} - \gamma^{e_4}\frac{1}{\not p_{14}}\gamma^{\mu}\frac{1}{\not p_{235}}\gamma^{e_5} + \gamma^{\mu}\frac{1}{\not p_{2345}}\gamma^{e_4}\frac{1}{\not p_{235}}\gamma^{e_5}\right) \\
&\quad + f^{aa_3a_4}T^{a_5}T^{a}\left(\gamma^{e_5}\frac{1}{\not p_{15}}\gamma^{e_4}\frac{1}{\not p_{1345}}\gamma^{\mu} - \gamma^{e_5}\frac{1}{\not p_{15}}\gamma^{\mu}\frac{1}{\not p_{234}}\gamma^{e_4} + \gamma^{\mu}\frac{1}{\not p_{2345}}\gamma^{e_5}\frac{1}{\not p_{234}}\gamma^{e_4}\right) \\
&\quad - f^{aa_3a_5}T^{a}T^{a_4}\left(\gamma^{e_5}\frac{1}{\not p_{135}}\gamma^{e_4}\frac{1}{\not p_{1345}}\gamma^{\mu} - \gamma^{e_5}\frac{1}{\not p_{134}}\gamma^{\mu}\frac{1}{\not p_{24}}\gamma^{e_4} + \gamma^{\mu}\frac{1}{\not p_{2345}}\gamma^{e_5}\frac{1}{\not p_{24}}\gamma^{e_4}\right)\Bigg\} v(p_2).
\end{aligned} \tag{18}$$

Next we consider the diagrams with only one 3-gluon vertex, i.e. classes a_1, a_2, b_1, b_2, c_1 and c_2 in the notation of appendix A. For this we need the contraction of the 3-gluon vertex with p_3.

$$
\begin{aligned}
& p_3^{e_3} \cdot V_3(p_{i3}, -p_i, -p_3, \alpha, \beta, e_3) \\
& \quad = p_3^{e_3} \cdot \left[g_{\alpha\beta}(2p_i + p_3)_{e_3} + g_{\beta e_3}(p_3 - p_i)_\alpha + g_{\alpha e_3}(-p_i - 2p_3)_\beta \right] \\
& \quad = 2g_{\alpha\beta} p_i \cdot p_3 - (p_{i3})_\alpha (p_{i3})_\beta + (p_i)_\alpha (p_i)_\beta . \qquad (19)
\end{aligned}
$$

In the sum $S_3 = p_3^{e_3} \cdot (a_1 + a_2 + b_1 + b_2 + c_1 + c_2)$ part of the terms cancel the r.h.s. of eq. (18). The remainder, i.e. the sum of (18) and S_3, is equal to

$$
\begin{aligned}
& p_3^{e_3} \cdot \sum (q\bar{q}3g - \text{graphs with at most one 3-gluon vertex}) \\
& \quad = p_3^{e_3} \cdot (I + II + III + IV + V + VI + a_1 + a_2 + b_1 + b_2 + c_1 + c_2) \\
& \quad = \bar{u}(p_1) \Bigg\{ i f^{a a_3 a_4} f^{a a_5 a_1} T^{a_1} \frac{p_{34}^{e_4}}{p_{34}^2} \left(\gamma^{e_5} \frac{1}{\not p_{1345}} \gamma^\mu - \gamma^\mu \frac{1}{\not p_{2345}} \gamma^{e_5} \right) \\
& \qquad + i f^{a a_5 a_3} f^{a a_4 a_1} T^{a_1} \frac{p_{35}^{e_5}}{p_{35}^2} \left(-\gamma^{e_4} \frac{1}{\not p_{1345}} \gamma^\mu + \gamma^\mu \frac{1}{\not p_{2345}} \gamma^{e_4} \right) \\
& \qquad + i f^{a a_4 a_5} f^{a a_3 a_1} T^{a_1} \frac{1}{p_{45}^2} \left(\gamma^\alpha \frac{1}{\not p_{1345}} \gamma^\mu - \gamma^\mu \frac{1}{\not p_{2345}} \gamma^\alpha \right) \cdot V_3(p_{45}, -p_5, -p_4, \alpha, e_5, e_4) \\
& \qquad + f^{a a_4 a_3} T^a T^{a_5} \frac{p_4^{e_4}}{p_{34}^2} \left(\not p_4 \frac{1}{\not p_{134}} \gamma^{e_5} \frac{1}{\not p_{1345}} \gamma^\mu - \not p_4 \frac{1}{\not p_{134}} \gamma^\mu \frac{1}{\not p_{25}} \gamma^{e_5} + \gamma^\mu \frac{1}{\not p_{2345}} \not p_4 \frac{1}{\not p_{25}} \gamma^{e_5} \right) \\
& \qquad + f^{a a_4 a_3} T^{a_5} T^a \frac{p_4^{e_4}}{p_{34}^2} \left(\gamma^{e_5} \frac{1}{\not p_{15}} \not p_4 \frac{1}{\not p_{1345}} \gamma^\mu - \gamma^{e_5} \frac{1}{\not p_{15}} \gamma^\mu \frac{1}{\not p_{234}} \not p_4 + \gamma^\mu \frac{1}{\not p_{2345}} \gamma^{e_5} \frac{1}{\not p_{234}} \not p_4 \right) \\
& \qquad + f^{a a_5 a_3} T^{a_4} T^a \frac{p_5^{e_5}}{p_{35}^2} \left(\gamma^{e_4} \frac{1}{\not p_{14}} \not p_5 \frac{1}{\not p_{1345}} \gamma^\mu - \gamma^{e_4} \frac{1}{\not p_{14}} \gamma^\mu \frac{1}{\not p_{235}} \not p_5 + \gamma^\mu \frac{1}{\not p_{2345}} \gamma_{e_4} \frac{1}{\not p_{235}} \not p_5 \right) \\
& \qquad + f^{a a_5 a_3} T^a T^{a_4} \frac{p_5^{e_5}}{p_{35}^2} \left(\not p_5 \frac{1}{\not p_{135}} \gamma^{e_4} \frac{1}{\not p_{1345}} \gamma^\mu - \not p_5 \frac{1}{\not p_{135}} \gamma^\mu \frac{1}{\not p_{24}} \gamma^{e_4} + \gamma^\mu \frac{1}{\not p_{2345}} \not p_5 \frac{1}{\not p_{24}} \gamma^{e_4} \right) \Bigg\} v(p_2) \\
& \qquad (20)
\end{aligned}
$$

Before we proceed with a_3, b_3 and c_3 which contain two structure constants, it is reasonable to subtract the ghost contribution with only one structure constant.

These are in the classes GI and GII and are of the following form:

$$p_4^{e_4}\cdot \mathrm{GI}(3,4) = f^{aa_3a_4}T^{a_5}T^{a}\frac{p_4^{e_4}}{p_{34}^2}\bar{u}(p_1)$$
$$\times\left(\gamma^{e_5}\frac{1}{\not p_{15}}\not p_3\frac{1}{\not p_{1345}}\gamma^{\mu}-\gamma^{e_5}\frac{1}{\not p_{15}}\gamma^{\mu}\frac{1}{\not p_{234}}\not p_3+\gamma^{\mu}\frac{1}{\not p_{2345}}\gamma^{e_5}\frac{1}{\not p_{234}}\not p_3\right)v(p_2). \tag{21}$$

The $\not p_3$ can be eliminated by writing $p_3 = p_{34} - p_4$ and then using eq. (17). The same is being done with GII(3,4). The sum of GI(3,4) and GII(3,4) is

$$p_4^{e_4}\cdot(\mathrm{GI}+\mathrm{GII})(3,4)$$
$$= f^{aa_3a_4}\frac{p_4^{e_4}}{p_{34}^2}\bar{u}(p_1)\Bigg\{T^{a_5}T^{a}\Bigg(-\gamma^{e_5}\frac{1}{\not p_{15}}\not p_4\frac{1}{\not p_{1345}}\gamma^{\mu}+\gamma^{e_5}\frac{1}{\not p_{15}}\gamma^{\mu}\frac{1}{\not p_{234}}\not p_4$$
$$-\gamma^{\mu}\frac{1}{\not p_{2345}}\gamma^{e_5}\frac{1}{\not p_{234}}\not p_4\Bigg)+T^{a}T^{a_5}\Bigg(-\not p_4\frac{1}{\not p_{134}}\gamma^{e_5}\frac{1}{\not p_{1345}}\gamma^{\mu}+\not p_4\frac{1}{\not p_{134}}\gamma^{\mu}\frac{1}{\not p_{25}}\gamma^{e_5}$$
$$-\gamma^{\mu}\frac{1}{\not p_{2345}}\not p_4\frac{1}{\not p_{25}}\gamma^{e_5}\Bigg)+if^{aa_5a_1}T^{a_1}\Bigg(\gamma^{e_5}\frac{1}{\not p_{1345}}\gamma^{\mu}-\gamma^{\mu}\frac{1}{\not p_{2345}}\gamma^{e_5}\Bigg)\Bigg\}v(p_2). \tag{22}$$

The $p_5^{e_5}\cdot(\mathrm{GI}+\mathrm{GII})(3,5)$ is obtained from eq. (22) by interchanging $4\leftrightarrow 5$. Both expressions are subtracted from the r.h.s. of eq. (20). This yields

$$p_3^{e_3}\cdot(\mathrm{I}+\mathrm{II}+\cdots+\mathrm{VI}+\mathrm{a}_1+\mathrm{a}_2+\cdots+\mathrm{c}_2)$$
$$-p_4^{e_4}\cdot(\mathrm{GI}+\mathrm{GII})(3,4)-p_5^{e_5}\cdot(\mathrm{GI}+\mathrm{GII})(3,5)$$
$$=\bar{u}(p_1)\Bigg\{if^{aa_3a_4}f^{aa_5a_1}T^{a_1}\frac{p_3^{e_4}}{p_{34}^2}\left(\gamma^{e_5}\frac{1}{\not p_{1345}}\gamma^{\mu}-\gamma^{\mu}\frac{1}{\not p_{2345}}\gamma^{e_5}\right)$$
$$+if^{aa_5a_3}f^{aa_4a_1}T^{a_1}\frac{p_3^{e_5}}{p_{35}^2}\left(-\gamma^{e_4}\frac{1}{\not p_{1345}}\gamma^{\mu}+\gamma^{\mu}\frac{1}{\not p_{2345}}\gamma^{e_4}\right)$$
$$+if^{aa_4a_5}f^{aa_3a_1}T^{a_1}\frac{1}{p_{45}^2}\left(\gamma^{\alpha}\frac{1}{\not p_{1345}}\gamma^{\mu}-\gamma^{\mu}\frac{1}{\not p_{2345}}\gamma^{\alpha}\right)$$
$$\times V_3(p_{45},-p_5,-p_4,\alpha,e_5,e_4)\Bigg\}v(p_2). \tag{23}$$

Let us denote in the following all terms proportional to $if^{aa_3a_4}f^{aa_5a_1}$ by ST_1, all terms proportional to $if^{aa_5a_3}f^{aa_4a_1}$ by ST_2 and all contributions proportional to $if^{aa_4a_5}f^{aa_3a_1}$ by ST_3. Contributions to ST_1 occur in a_3, GV(3,4) and GIII (3,5) and in the first term in eq. (23), similarly for ST_2 and ST_3. In total these terms are

$$\begin{aligned}
ST_1 &= p_3^{e_3}\cdot a_3 - p_4^{e_4}\cdot GV(3,4) - p_5^{e_5}\cdot GIII(3,5) + (\text{first term in eq. (23)}),\\
ST_2 &= p_3^{e_3}\cdot c_3 - p_4^{e_4}\cdot GIII(3,4) - p_5^{e_5}\cdot GV(3,5) + (\text{second term in eq. (23)}),\\
ST_3 &= p_3^{e_3}\cdot b_3 - p_4^{e_4}\cdot GIV(3,4) - p_5^{e_5}\cdot GIV(3,5) + (\text{third term in eq. (23)}). \qquad (24)
\end{aligned}$$

The explicit evaluation of ST_1, ST_2 and ST_3 gives

$$\begin{aligned}
ST_1 = {} & if^{aa_5a_1}f^{a_1a_3a_4}T^a\frac{1}{p_{345}^2}\bar u(p_1)\left(\gamma^\alpha\frac{1}{\not p_{1345}}\gamma^\mu-\gamma^\mu\frac{1}{\not p_{2345}}\gamma^\alpha\right)v(p_2)\\
&\times\Bigg\{-\frac{p_3^{e_3}}{p_{34}^2}V_3(p_{345},-p_5,-p_{34},\alpha,e_5,\beta)V_3(p_{34},-p_4,-p_3,\beta,e_4,e_3)\\
&\quad -p_3^{e_3}\left(g_\alpha^{e_4}g_{e_3}^{e_5}-g_{\alpha e_3}g^{e_4e_5}\right)-\frac{p_4^{e_4}}{p_{34}^2}p_3^\beta V_3(p_{345},-p_5,-p_{34},\alpha,e_5,\beta)\\
&\quad +\frac{p_5^{e_5}}{p_{34}^2}p_3^{e_4}p_{34\alpha}-\frac{p_{345}^2}{p_{34}^2}p_3^{e_4}g_\alpha^{e_5}\Bigg\} \qquad (25)\\
ST_2 = {} & if^{aa_4a_1}f^{a_1a_5a_4}T^a\frac{1}{p_{345}^2}\bar u(p_1)\left(\gamma^\alpha\frac{1}{\not p_{1345}}\gamma^\mu-\gamma^\mu\frac{1}{\not p_{2345}}\gamma^\alpha\right)v(p_2)\\
&\times\Bigg\{-\frac{p_3^{e_3}}{p_{35}^2}V_3(p_{345},-p_4,-p_{35},\alpha,e_4,\beta)V_3(p_{35},-p_3,-p_5,\beta,e_3,e_5)\\
&\quad -p_3^{e_3}\left(g_{\alpha e_3}g^{e_4e_5}-g_\alpha^{e_5}g_{e_3}^{e_4}\right)+\frac{p^{e_5}}{p_{35}^2}p_3^\beta V_3(p_{345},-p_4,-p_{35},\alpha,e_4,\beta)\\
&\quad -\frac{p_4^{e_4}}{p_{35}^2}p_3^{e_5}p_{35\alpha}+\frac{p_{345}^2}{p_{35}^2}p_3^{e_5}g_\alpha^{e_4}\Bigg\}. \qquad (26)\\
ST_3 = {} & if^{aa_3a_1}f^{a_1a_4a_5}T^a\frac{1}{p_{345}^2}\bar u(p_1)\left(\gamma^\alpha\frac{1}{\not p_{1345}}\gamma^\mu-\gamma^\mu\frac{1}{\not p_{2345}}\gamma^\alpha\right)v(p_2)\\
&\times\Bigg\{-\frac{p_3^{e_3}}{p_{45}^2}V_3(p_{345},-p_3,-p_{45},\alpha,e_3,\beta)V_3(p_{45},-p_5,-p_4,\beta,e_5,e_4)\\
&\quad -p_3^{e_3}\left(g_\alpha^{e_5}g_{e_3}^{e_4}-g_\alpha^{e_4}g_{e_3}^{e_5}\right)-\frac{p_{345}^2}{p_{45}^2}V_3(p_{45},-p_5,-p_4,\alpha,e_5,e_4)\\
&\quad -\frac{p_4^{e_4}}{p_{45}^2}p_{45}^{e_5}p_{3\alpha}+\frac{p_5^{e_5}}{p_{45}^2}p_{45}^{e_4}p_{3\alpha}\Bigg\}. \qquad (27)
\end{aligned}$$

It is shown that the curly brackets in eqs. (25)–(27) coincide. Using the definitions for V_3 the curly bracket can be reduced further and we obtain

$$
\begin{aligned}
& p_3^{e_3} \cdot \sum (\mathrm{q\bar{q}3g - graphs}) - p_4^{e_4} \cdot \mathrm{ghost}(3,4) - p_5^{e_5} \cdot \mathrm{ghost}(3,5) \\
& \quad = i\left(f^{aa_5a_1} f^{a_1a_3a_4} + f^{aa_4a_1} f^{a_1a_3a_5} + f^{aa_3a_1} f^{a_1a_4a_5} \right) \\
& \qquad \times T^a \frac{1}{p_{345}^2} \bar{u}(p_1) \left(\gamma^\alpha \frac{1}{\not{p}_{1345}} \gamma^\mu - \gamma^\mu \frac{1}{\not{p}_{2345}} \gamma^\alpha \right) v(p_2) \\
& \qquad \times \left[-g^{e_4e_5}(p_4 - p_5)_\alpha + g_\alpha^{e_4}(p_5^{e_5} + p_3^{e_5} + 2p_4^{e_5}) - g_\alpha^{e_5}(p_4^{e_4} + p_3^{e_4} + 2p_5^{e_4}) \right] = 0
\end{aligned}
\tag{28}
$$

because of the Jacobi identity for the product of structure constants. This shows that the STI is fulfilled. Therefore, the ghost contributions have the correct form.

As a last point in this appendix we report the colour factors for the ghost diagrams. For example, for the diagram ghost(3,4) the colour factor is $\mathrm{GI} = f^{aa_3a_4} T^{a_5} T^{a_3}$. Then the colour factor for the squared graph is

$$
\mathrm{GI} \cdot \mathrm{GI}^* = f^{ba_3a_4} f^{aa_3a_4} \mathrm{Tr}(T^{a_5} T^a T^b T^{a_5}) = N_c^2 C_F^2 = C F_5 . \tag{29}
$$

All other products are calculated in the same way. The results are collected in table 4. They are also valid for all the other ghost sets ghost(i, j).

We wish to thank F.A. Berends and H. Kuijf for explaining their method. Furthermore, we gratefully acknowledge that they provided us with preliminary partial results [9] for the purpose of comparison.

References

[1] B. Naroska, Phys. Rep. 148 (1987) 67;
W. de Boer, SLAC-PUB-4428 (1987);
P. Mättig, Int. J. Mod. Phys. A3 (1987) 1
[2] W. Bartel et al., Z. Phys. C33 (1986) 23;
S. Bethke, Habilitationsschrift, University of Heidelberg, 1987 (unpublished);
W. Braunschweig et al., Phys. Lett. B 214 (1988) 286;
I.H. Park et al., KEK-report 88-45, AMY-report 88-08
[3] S.G. Gorishny, A.L. Kataev and S.A. Larin, Phys. Lett. B 212 (1988) 238
[4] N.K. Falck, D. Graudenz and G. Kramer, Phys. Lett. B220 (1989) 299
[5] N.K. Falck, D. Graudenz and G. Kramer, DESY report 89-046 (1989)
[6] R. Cutler and D. Sivers, Phys. Rev. D17 (1978) 96;
T. Gottschalk and D. Sivers, Phys. Rev. D21 (1980) 102

[7] A. Ali, J.G. Körner, Z. Kunzt, E. Pietarienen, G. Kramer, G. Schierholz and J. Willrodt, Phys. Lett. B82 (1979) 285; Nucl. Phys. B167 (1980) 454;
L. Clavelli and G. van Gehlen, Phys. Rev. D27 (1983) 1495;
D. Dankaert et al., Phys. Lett. B114 (1982) 203
[8] Wang-Chuang Kuo, David Slaven and Bing-Lin Young, Phys. Rev. D37 (1988) 233
[9] K. Hagiwara and D. Zeppenfeld, Nucl. Phys. B313 (1989) 560; and F.A. Berends, W.T. Giele and H. Kuijf, University of Leiden preprint, for calculational procedures based on helicity amplitudes and S. J. Parke and T.R. Taylor, Phys. Lett. B 157 (1985) 81;
M. Mangano and S.J. Parke, Nucl. Phys. B299 (1988) 673 for supersymmetric techniques
[10] K.J.F. Gaemers and J.A.M. Vermaseren, Z. Phys. C7 (1980) 81
[11] G. Kramer, Springer tracts in modern physics, Vol. 102 (Springer, Berlin, 1984)